Simultaneous surface and volumetric registration using harmonic maps

Anand A. Joshi[a], David W. Shattuck[b], Paul M. Thompson[b] and Richard M. Leahy[a]

[a]University of Southern California, Los Angeles, CA 90089, USA;
[b]University of California, Los Angeles, CA 90095, USA

ABSTRACT

Inter-subject analysis of anatomical and functional brain imaging data requires the images to be registered to a common coordinate system in which anatomical features are aligned. Intensity-based volume registration methods can align subcortical structures well, but the variability in sulcal folding patterns typically results in misalignment of the cortical surface. Conversely, surface-based registration using sulcal features can produce excellent cortical alignment but the mapping between brains is restricted to the cortical surface. Here we describe a method for volumetric registration that also produces a one-to-one point correspondence between cortical surfaces. This is achieved by first parameterizing and aligning the cortical surfaces. We then use a constrained harmonic mapping to define a volumetric correspondence between brains. Finally, the correspondence is refined using an intensity-based warp. We evaluate the performance of our proposed method in terms of the inter-subject alignment of expert-labeled sub-cortical structures after registration.

Keywords: Volumetric registration, Harmonic mappings.

1. INTRODUCTION

Inter-subject studies for detecting systematic patterns of brain structure and function in human populations require that the data first be transformed to a common coordinate system in which anatomical structures are aligned. Similarly, inter-subject longitudinal studies or group analyses of functional data also require that the images first be anatomically aligned. Such an alignment is commonly performed either with respect to the entire volumetric space[1] or is restricted to the cortical surface.[2] Here we describe an approach to brain image registration based on harmonic maps that combines these two approaches producing a volumetric alignment in which there is also a one-to-one correspondence between points on the two cortical surfaces.

Volumetric brain image registration methods[3–10] try to align intensity values and landmarks by finding a diffeomorphism between the two brain image volumes by finding a deformation field which aligns one volume to another. In addition to the intensity, additional information such as landmark points, curves and surfaces can be incorporated as additional constraints in an intensity-based warping method.[2, 11–16] Landmarks, curves[16] and image matching[15] have been applied in a hierarchical manner in a large deformation framework ensuring generation of diffeomorphisms.[17, 18] The volume registration methods provide a good registration of subcortical structures, but do not provide an accurate cortical alignment. While the regions of cortical grey matter exhibit reasonably good correspondence between the two images, the cortical surfaces themselves do not align well. Since cytoarchitectural and functional parcellation of the cortex is intimately related to the folding of the cortex, it is important when comparing cortical anatomy and function in two or more subjects that the surfaces are aligned. For this reason, there has been an increasing interest in alignment of surfaces rather than volumes.

Various surface-based techniques have been developed for inter-subject registration of two cortical models. One class of techniques involves flattening the two cortical surfaces to a plane or to a sphere[19] using mechanical models or variational methods and then analyzing the data in the common flat space.[20] Other surface based techniques work in the surface geometry itself rather than a plane or a sphere and choose to account for the surface

metric in the inter-subject registration.[21, 22] The advantage of such techniques is that they produce registration results that are independent of the intermediate flat space (or, equivalently, the specific parameterization of the cortex) resulting in a more consistently accurate registration throughout the cortex. These approaches involve manually delineated sulcal landmark matching[22] in the intrinsic surface geometry. While some progress has been made recently towards automating the matching process using mutual information[23] or optical flows of mean-curvature images in the surface parameter space,[24, 25] fully automatic alignment of high resolution cortical surfaces remains a challenging problem.

While the volume registration methods described above do not provide suitable cortical alignment, the cortical registration methods do not define any volumetric correspondence. Registration methods such as the Hierarchial Attribute Matching Mechanism for Image Registration (HAMMER) algorithm[26, 27] incorporate surface as well as volume information in the alignment procedure. For brain images, the desired deformation fields need to be obtained incrementally by using large deformation or fluid models[28, 29] and hence are computationally expensive. Additionally, accurate alignment of the cortical surface as well as the cortical volume remains a challenging task mainly due to the complex folding pattern variability of the cortex.

We present a registration method which combines surface as well as a volume alignment methods to perform the final normalization. We start by aligning the cortical surfaces, semi-automatically, by using sulcal landmarks. Then we use harmonic maps to extrapolate this surface mapping to the entire cortical volume. Harmonic maps are suitable for this task since they are bijective provided that the boundary (cortical surface in this case) is mapped bijectively.[30] Finally, an intensity based volumetric registration refines this correspondence to align subcortical structures.

2. PROBLEM STATEMENT AND FORMULATION

Given two 3D manifolds M and N representing subject and template brain volumes, with boundaries ∂M and ∂N representing corresponding cortical surfaces, we want to find a map from M to N such that ∂M, the surface of M, maps to ∂N, the surface of N, and the intensities of the images in the interior of M and N are matched. The boundaries, ∂M and ∂N, representing the cortical surfaces of the two brain volumes are assumed to have a spherical topology. We solve the mapping problem in three steps:

1. Surface matching which computes a map between ∂M and ∂N - subject and template surfaces, with sulcal alignment constraints. This is performed by using thin-plate spline registration in the intrinsic surface geometry as discussed in Section 3.

2. Extrapolation of the surface map to the entire cortical volume such that the cortical surfaces remain aligned. This is done by computing a harmonic map between M and N subject to surface matching constraints. As we describe in Section 4.3, an intermediate spherical representation is used to facilitate enforcement of this constraint. We note also that while the sulci are constrained to remain in correspondence, the cortical surfaces can flow with respect to each other when computing the volume harmonic map provided we retain the one-to-one mapping between ∂M and ∂N;

3. Refinement of the harmonic map on the interiors of M and N to improve intensity alignment leading to better registration of subcortical structures. The third step is describe in Section 5.

3. SURFACE MATCHING

The first step of our procedure is extraction and registration of subject and template cortical surfaces. Assuming as input, two T1 weighted MR volumes corresponding to the subject, cortical surfaces are extracted from volume images for the two brains using the BrainSuite software.[31] BrainSuite includes a six stage cortical modeling sequence. First the brain is extracted from the surrounding skull and scalp tissues using a combination of edge detection and mathematical morphology. Next the intensities of the magnetic resonance images (MRI) are corrected for shading artifacts. Each voxel in the corrected image is labeled according to tissue type using a statistical classifier. Co-registration to a standard atlas is then used to automatically identify the white matter volume, fill ventricular spaces and remove the brain stem and cerebellum, leaving a volume whose surface

represents the outer white-matter surface of the cerebral cortex. It is likely that the tessellation of this volume will produce surfaces with topological handles. Prior to tessellation, these handles are identified and removed automatically using a graph based approach. A tessellated isosurface of the resulting mask is then extracted to produce a genus zero surface which is subsequently split into two cortical hemispheres. These extracted surfaces are hand labeled with 23 major sulci on each cortical hemisphere according to a sulcal labeling protocol with established intra- and inter-rater reliability.[31] This protocol specifies that sulci do not intersect and that individual sulci are continuous curves that are not interrupted. If interruptions are present, the human raters specify the path across any interrupting gyri. We note that the procedure implemented in BrainSuite to find the cortical surface uses the inner grey/white boundary of cortex as the surface. Consequently the images shown here do not include cortical grey matter but are restricted to white matter, ventricles and subcortical grey matter. The sulcal landmarks and triangulated mesh models of the subject and template cortical surfaces are used for the surface registration procedure which sets up a point correspondence between the two surface.

We use a thin-plate spline based surface registration method as we have previously described.[22] This method produces a bijective point correspondence between the two cortical surfaces by aligning their coordinate systems. This is done by first mapping the two surfaces to unit squares using p-harmonic energy minimization and then aligning their sulcal landmarks by computing a coordinate deformation field to align the sulcal coordinates. The field is regularized using the intrinsic thin-plate bending energy computed using the covariant bi-harmonic equation. The resulting deformation field defines a one to one correspondence between the subject and template surfaces. We refer the reader to Joshi et al.[22] for a more detailed description of this method. We note that any of the landmark based or automated surface registration algorithms[20, 23–25, 32–34] could also be used for this step.

4. HARMONIC MAPPING

The surface registration procedure as described in Section 3 sets up a point to point correspondence between the subject and template cortical surfaces. Extrapoliating this correspondence from the boundary of the cortical volume to the entire cortical volume in a one-to-one manner is challenging due to the convoluted nature of the cortex. We propose that 3D harmonic maps are attractive for this purpose due to their tendency to be bijective if the boundary (cortical surface) are mapped bijectively.[35]

This section describes the harmonic mapping between two 3D volumes. A computational scheme for extending the surface maps to the volumes is also described. We refer readers to Jost[35] for basic properties of harmonic maps.

4.1. Mathematical Formulation

Let $u : M \to N$ be a C^∞ map from a 3-dimensional Riemannian manifold (M, g) to an 3-dimensional Riemannian manifold (N, h) where g and h are Riemannian metrics for M and N respectively. Riemannian metric defines an inner product at every point in the manifold and thus helps in defining the notion of distance on the manifold.[35] Let $\{g_{ij}; i, j \in \{1, 2, 3\}\}$ denote components of the Riemannian metric tensor g and $\{h_{\alpha\beta}; \alpha, \beta \in \{1, 2, 3\}\}$ denote the components of the Riemannian metric tensor h. The inverse of the metric $g = \{g_{ij}\}$ is denoted by $\{g^{ij}\}$. Let (x^1, x^2, x^3) and (u^1, u^2, u^3) be local coordinates for x and $u(x)$ respectively. The *mapping energy* in coordinate form[36] is given by:

$$E(u) = \frac{1}{2} \int_M \sum_{i,j=1}^{3} \sum_{\alpha,\beta=1}^{3} g^{ij}(x) h_{\alpha\beta}(u(x)) \frac{\partial u^\alpha(x)}{\partial x^i} \frac{\partial u^\beta(x)}{\partial x^j} d\mu_g, \tag{1}$$

where the integration is over the manifold M with respect to the intrinsic measure $d\mu_g$ induced by its Riemannian metric g. A *harmonic map* from (M, g) to (N, h) is defined to be a critical point of the mapping energy $E(u)$.

A number of existence, uniqueness, and regularity results have been proven for harmonic maps.[37] Eells and Sampson[38] proved the existence of a harmonic map from any compact Riemannian manifold to a compact Riemannian manifold of non-positive sectional curvature. Hamilton[30] generalized this result to manifolds with boundaries. In medical imaging, harmonic mappings and p-harmonic mappings, their generalized counterparts, have been used for various applications such as surface parameterization and registration[39] and image smoothing.[40] Wang et al.[41] describe a method for volumetric mapping of the brain to the unit ball $B(0, 1)$. Here we use harmonic maps to align two brain volumes so that both the brain volumes and cortical surfaces are aligned.
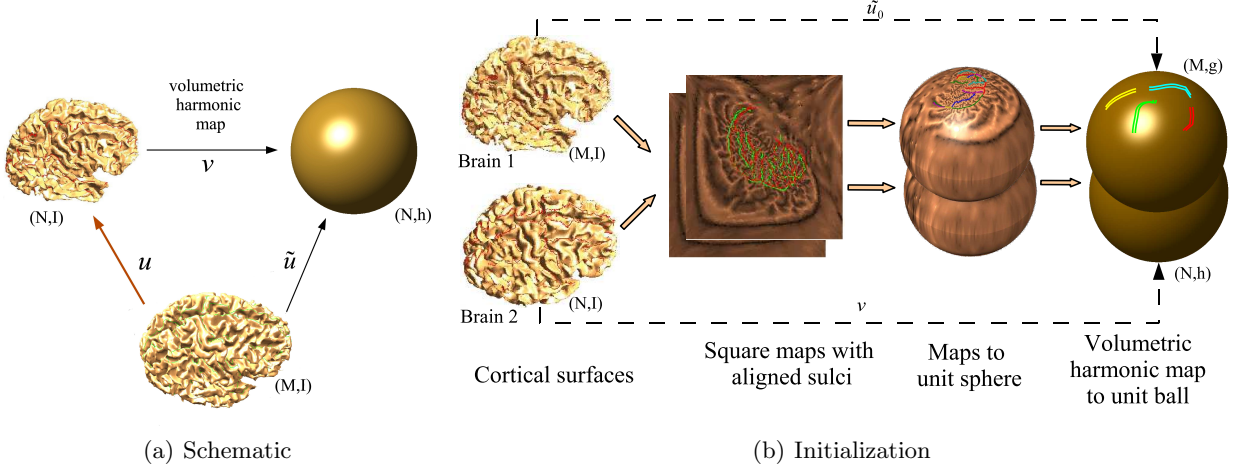
(a) Schematic   (b) Initialization

Figure 1. (a) Illustration of our general framework for surface-constrained volume registration. We first compute the map v from brain manifold (N, I) to the unit ball to form manifold (N, h). We then compute a map $\tilde{u}$ from brain (M, I) to (N, h). The final harmonic map from (M, I) to (N, I) is then given by $u = v^{-1} \circ \tilde{u}$. (b) The initialization for the mapping procedure. First we generate flat square maps of the two brains, one for each hemisphere, with sulci aligned. Then we map the squares corresponding to each hemispheres to a disk and project the disks onto the unit sphere. We then generate a volumetric maps from each of the brains to the unit ball. Since all these maps are bijective, the resulting map gives us a bijective point correspondence between the two brains. However, this correspondence is not optimal with respect to the harmonic energy of maps from the first brain to the second, but is used as an initialization for minimization of (3)

One approach to the mapping problem is to first align the surfaces of the two manifolds and then align the volumes in their interiors while keeping the surfaces fixed. However, fixing the surface correspondence before aligning the volumes will result in a suboptimal mapping with respect to the 3D mapping energy. To overcome this problem and compute an optimal mapping for the surface as well as the interior, we instead allow the surface M to flow within the surface of N when computing the map. The only constraints placed on the surfaces are that the maps are aligned at a set of user defined sulcal landmarks. This less restrictive surface mapping constraint cannot be formulated directly in the ambient Euclidean 3D space since there is no analytical expression for the surfaces, although this could be accomplished without parameterizing the surface using a level set approach.[32, 40] Here we use an intermediate representation for the manifolds which allows us to enforce the boundary matching constraint while allowing one boundary to flow within the other. We achieve this by first computing a map $v : N \to B(0, 1)$ as described below. This mapping to the unit ball results in a non-Euclidean representation of N thus requiring the use of Riemannian metric in computing the harmonic map. The Riemannian metric $h = \{h_{\alpha\beta}\}$ associated with this representation is given by

$$h_{\alpha\beta} = \sum_{i=1}^{3} \frac{\partial x^i}{\partial v^\alpha} \frac{\partial x^i}{\partial v^\beta}. \tag{2}$$

Now instead of needing to directly compute the harmonic map $u : (M, I) \to (N, I)$, we instead find the harmonic map $\tilde{u} : (M, I) \to (N, h) \approx B(0, 1)$ subject to the constraint that the cortical surface ∂M maps to the spherical boundary of the unit ball, as illustrated in Fig. 1.

The harmonic mapping problem now becomes:

$$\tilde{u} = \arg\min_{\gamma} \int_M \sum_{i=1}^{3} \sum_{\alpha,\beta=1}^{3} h_{\alpha\beta}(\gamma(x)) \left(\frac{\partial \gamma^\alpha(x)}{\partial x^i} \right) \left(\frac{\partial \gamma^\beta(x)}{\partial x^i} \right) d\mu_g \tag{3}$$

subject to $\|\tilde{u}(x)\|^2 = 1$ for $x \in \partial M$, the surface of M. Note that this constraint allows the surface map to flow within the spherical boundary. While we want to allow one surface to flow with respect to the other, we

also want to constrain the maps so that predefined sulcal landmarks, a user-defined set of sampled curves, are aligned. To achieve this we impose the additional constraints that $\tilde{u}(c) = u_c$ for $c \in M_c$ where M_c are the set of sulcal landmark points in M and u_c are the locations of the homologous landmarks in (N, h).

4.2. Initialization Procedure

Because the minimization problem is nonlinear, it is important to have a good initial estimate of the map $\tilde{u}$ in order to achieve convergence in a reasonable amount of time. We therefore generate an initial estimate $\tilde{u}_0$ of $\tilde{u}$ by also computing a map of the second manifold (M, I) to the unit ball, just as we do for the first manifold (N, I) (Fig. 1). To compute mappings of brain manifolds to the unit ball, we first compute a mapping of the surfaces to the unit sphere with sulcal alignment as described in Section 3. To map the interior of the manifold (N, I) to the interior of the unit ball $B(0, 1)$, the mapping energy

$$E(v) = \int_M |\nabla v|^2 dV \tag{4}$$

is minimized to get v (Fig. 1) with the constraint that the surface ∂N maps to the unit sphere, the boundary of $B(0, 1)$. Here ∇ is the usual gradient operator in $3D$ Euclidean space and dV is the volume integral.[41] Similarly, in order to map the given cortical brain volume M to the unit ball, we minimize the mapping energy subject to the constraint that the surface of M maps to the surface of the unit ball using the point-to-point correspondence defined by the surface alignment. The minimization is computed using numerical integration over the voxel lattice and finite differences to approximate the gradients in (4). The resulting discretized cost function is minimized by conjugate gradient. The initialization procedure is illustrated in Fig. 1.

4.3. Harmonic Mapping Between the Two Brains

The initialization procedure results in maps u_0 from (M, I) and v from (N, I) to the unit ball such that the sulci on the cortical surface align on the unit sphere, the boundary of the unit ball. Since the map v is bijective, we can treat the unit ball as a coordinate system for the manifold N. The manifold N with the unit ball coordinates is denoted by (N, h). The $\tilde{u}_0$ from M to the unit ball is used to initialize the desired map $\tilde{u}$ from (M, I) to (N, h). With this initialization, we then compute the 3D harmonic map by minimizing (3) to obtain the desired harmonic map. The optimization problem is solved using numerical integration and finite difference operators, in this case accounting for the metric h when computing derivatives. In this mapping, the location of the sulci in M are constrained using their initial mappings $\tilde{u}_0$ computed when flattening and matching the cortical surfaces. Other points within the brain are allowed to move freely to minimize the harmonic energy, subject to the constraint that all points on the surface map to $\|\tilde{u}\|^2 = 1$, which is achieved by adding a penalty function to the discretized form of (3).

4.4. Implementation

4.4.1. Computation of Metric

The metric $h_{ij}(x), x \in N$ is associated with the unit ball coordinates $B(0, 1)$ given to N by the map $v = (v^1, v^2, v^3)$ (Fig. 1). It is given by $h_{\alpha\beta}(x) = \sum_{i=1}^{3} \frac{\partial x^i}{\partial v^\alpha} \frac{\partial x^i}{\partial v^\beta}$ with $\alpha, \beta \in \{1, 2, 3\}$ at $x = (x^1, x^2, x^3)$. Note that although $x \in N$ is in the regular grid, $v(x) \in B(0, 1)$ is not necessarily so, and hence computation of partial derivatives with respect to v directly is difficult. In order to compute $\frac{\partial v^\alpha}{\partial x^i}$, first compute $\frac{\partial v^\gamma}{\partial x^j}$ using finite differences and then use the chain rule identity $\sum_{\gamma=1}^{3} \frac{\partial x^i}{\partial v^\gamma} \frac{\partial v^\gamma}{\partial x^j} = \frac{\partial x^i}{\partial x^j} = \delta^i_j$ to solve for $\frac{\partial v^\gamma}{\partial x^j}$. The metric h_{ij} is computed by substituting these partial derivatives in the above equation.

4.4.2. Harmonic mapping

The harmonic mapping procedure can now be summarized as follows:

1. Align the surfaces of both the brains M and N as described in Section 3.

2. Map the unit squares to unit disks by the transformation $(x, y) \rightarrow (\frac{x}{\sqrt{x^2+y^2}}, \frac{y}{\sqrt{x^2+y^2}})$ and then project them onto two hemispheres using $(x, y) \rightarrow (x, y, 1 \pm \sqrt{x^2 + y^2})$.

3. Using this mapping of the cortical surface to the unit sphere as the boundary condition, generate a volumetric harmonic map of M and N to the unit ball $B(0,1)$ to get maps $\tilde{u}_0$ and v respectively as described in Section 4.2.

4. Compute the metric h associated with the unit ball $B(0,1)$ coordinates of N.

5. Minimize (3) holding the matched sulci fixed, and letting the cortical surface ∂M slide along the unit spherical boundary of the unit ball. This is done by minimizing (3) with the constraint that $\|\tilde{u}(x)\|^2 = 1$ for $x \in \partial M$ and $\tilde{u}(c) = \tilde{u}_0(c)$ for $c \in M_c$ where $M_c \subset M$ denotes the set of sulcal points on M.

6. Compute the deformation vector field $u(x) - x$ where $u = v^{-1} \circ \tilde{u}$ and apply this to map brain volume M to N. Trilinear interpolation is used for this deformation.

5. VOLUMETRIC INTENSITY REGISTRATION

The harmonic surface constrained volume alignment procedure described above produces a bijective mapping between the two brain volumes. However, it only uses the shape and does not use the MRI intensity values in the alignment method. Using this additional information, the alignment of subcortical structures within the brains can be improved further. In order to compute this refinement we use a linear elastic registration method as described below.

Let $f_M(x)$ denote the MRI intensity value at location $x = (x_1, x_2, x_3)^t$ for the brain M and let $f_N(x)$ denote the MRI intensity value at location $x = (x_1, x_2, x_3)^t$ for the brain N. In order to find a smooth deformation field $d = (d_1, d_2, d_3)^t$ such that the mean squared error between MRI intensity values of the two brains $f_M(x+d)$ and $f_N(x)$ is minimized, we minimize the cost function

$$C(d) = \|Ld\|^2 + \alpha\|f_M(x+d) - f_N(x)\|^2 \tag{5}$$

$$\text{subject to } d(s) = 0 \text{ for } s \in \partial M \tag{6}$$

where $L = \nabla^2 + \mu\nabla(\nabla\cdot)$ denotes the Cauchy-Navier elasticity operator in M. By imposing the constraint (6) on the deformation field, we ensure that the surface alignment is not affected. Assuming that the deformation d is small compared to the rate of change of f_M, then using a Taylor series approximation, we have $f_M(x+d) \approx f_M(x) + \nabla f_M(x) \cdot d$. Substituting this approximation in (5) and (6), we get

$$C(d) \approx \|Ld\|^2 + \alpha\|\nabla f_M(x) \cdot d(x) + f_M(x) - f_N(x)\|^2 \tag{7}$$

$$\text{subject to } d(s) = 0 \text{ for } s \in \partial M \tag{8}$$

Note that this is a quadratic cost function and can be minimized by the conjugate gradient method. We use a preconditioned conjugate gradient method with Jacobi preconditioner for this purpose.

This final refinement completes the surface-constrained registration procedure. While there are several steps required to complete the registration, each step can be reduced to either a surface or a volume mapping cast as an energy minimization problem, possibly with constraints, and can be effectively computed using a preconditioned conjugate gradient method, so that the entire procedure can be completed efficiently.

6. RESULTS AND VALIDATION

In this section we demonstrate the application of the surface constrained registration procedure to T1-weighted MR brain images. The labeled brain data was obtained from the IBSR dataset at the Center for Morphometric Analysis at Massachusetts General Hospital. This consists of T1-weighted MR images with $1.5mm$ slice thickness as well as expert segmentations of 43 individual structures. The cortical masks were obtained and their topology corrected using the BrainSuite software as described in Sec. 3. The cortical surfaces were then interactively labelled with 23 sulcal curves on each hemisphere using a standard labeling protocol.[42] Our registration algorithm was applied by performing surface matching, harmonic mapping and volumetric intensity registration as described above. Shown in Fig. 6 are three orthogonal views of a subject before and after alignment to the template image. Note that before alignment the surfaces of the subject and template are clearly different, while after matching
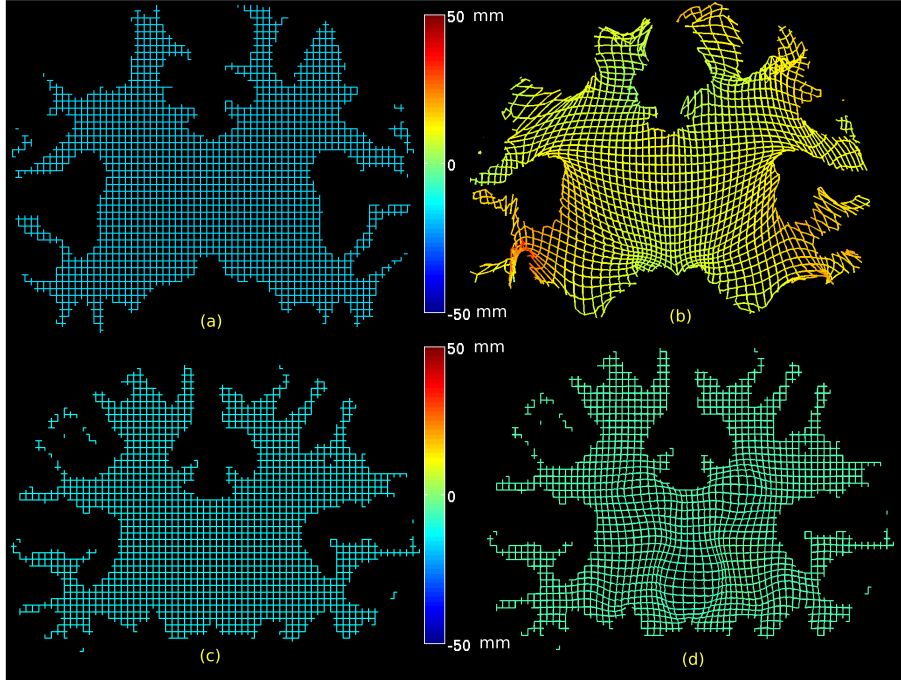
Figure 2. Illustration of the effects of the two stages of volumetric matching is shown by applying the deformations to a regular mesh representing one slice. Since the deformation is in 3D, the third in-paper value is represented by color. (a) Regular mesh representing one slice in the subject; (b) the regular mesh warped by the harmonic mapping which matches the subject cortical surface to the template cortical surface. Note that deformation is largest near the surface since the harmonic map is constrained only by the cortical surface; (c) Regular mesh representing one slice in the harmonically warped subject; (d) the intensity-based refinement now refines the deformation of the template to improve the match between subcortical structures. In this case the deformation is constrained to zero at the boundary and changes re confined to the interior of the volume.

the subject surface almost exactly matches the morphology of that of the template. However, since at this point we do not take the image intensities into account, the interior structures are somewhat different. Following the final intensity-based alignment procedure the interior structures, such as the ventricles better match those of the template.

There is no gold standard for evaluating the performance of registration algorithms such as the one presented here. However, there are several properties that are desirable for any such surface and volume registration algorithm.For evaluating the quality of our registration results is based on the following two desirable features:

1. Alignment of the cortical surface and sulcal landmarks. We expect the sulcal landmarks to be accurately aligned after registration and for the two surfaces to coincide.

2. Alignment of subcortical structures. We also expect the boundary of subcortical structures (thalamus, lateral ventricles, corpus callosum) to be better aligned after coregistration than before.

In order to evaluate the performance with respect to 1 we used a set of 6 MR volumes on which we had labeled 23 sulci in each hemisphere. The pairs of cortical volumes were registered using our method as described above. For comparison we used a 5th order polynomial intensity-driven warp computed using the AIR software.[5, 43] We also compared performance with the HAMMER[26, 27] algorithm. HAMMER is an automated method for volume registration which is able to achieve improved alignment of geometric features by basing the alignment on an attribute vector that includes a set of geometric moment invariants rather than simply the voxel intensities. We note that since our approach uses explicitly labelled sulci we can expect better performance than either AIR
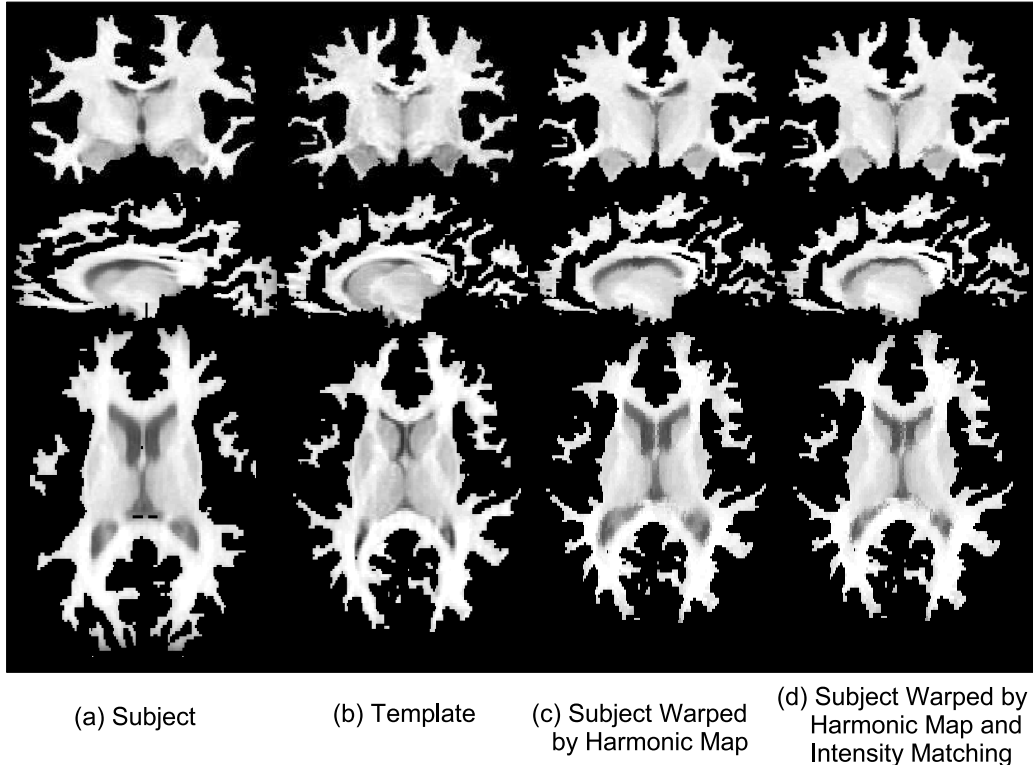
| (a) Subject | (b) Template | (c) Subject Warped by Harmonic Map | (d) Subject Warped by Harmonic Map and Intensity Matching |

Figure 3. Examples of surface constrained volumetric registration. (a) Original subject volume; (b) original template; (c) registration of subject to template using surface constrained harmonic mapping, note that the surface matches that of the template; (d) intensity-based refinement of the harmonic map of subject to template to complete registration procedure

or HAMMER in terms of the alignment of these features. However, AIR and HAMMER provide a basis for comparison from some of the most widely used and best performing algorithms for volumetric registration.

We measured the mean squared distance between pairs of homologous landmarks corresponding to uniform samples along each of the 23 labeled sulci. This procedure was repeated for each of the 30 possible pairwise registrations of two from six brains and computed the average mean squared distance over all registrations. We found that the mean squared distance (misalignment) between the respective sulcal landmarks was $11mm$ for HAMMER registration and $3.2mm$ after our cortically constrained method. The difference in performance is not suprising but reflects the fact that our approach explicitly constrains these sulcal features to match, which HAMMER does not as described above.

For 2 we used manually labeled brain data from the IBSR database at the Center for Morphometric Analysis at Massachusetts General Hospital (http://www.cma.mgh.harvard.edu/ibsr/). These data include volumetric MR data and hand segmented and labeled structures.To evaluate accuracy, we computed the Dice coefficients for each subcortical structure, where the structure names and boundaries were taken from the IBSR database. Dice coefficient which measures overlap between two regions, say region P and region Q, is defined as $\frac{2|P \cap Q|}{|P|+|Q|}$ where $|\cdot|$ denotes size of the region. A comparison of the Dice coefficients is shown in Table 6, where we show Dice coefficients for our method before and after application of the final intensity-based alignment step. It can be noted that our method produces comparable volumetric subcortical alignment as HAMMER, while performing better cortical surface registration. This study shows that our method is able to simultaneously align sulcal landmarks, the cortical surface, and the interior intensity structures in the brain, with reasonable accuracy. Larger scale validation is still needed.

The examples shown here demonstrate the cortical matching properties and the ability to also align sub-

Table 1. Comparison of Dice coefficients

Subcortical Structure	AIR	Harmonic	HAMMER	Harmonic with intensity
Left Thalamus	0.6588	0.4903	0.7303	0.5565
Left Caudate	0.4426	0.4804	0.5688	0.5747
Left Putamen	0.4079	0.3509	0.4905	0.5060
Left Hippocampus	0.4676	0.2590	0.3916	0.2639
Right Thalamus	0.6326	0.5030	0.7495	0.6071
Right Caudate	0.3671	0.3997	0.5098	0.4885
Right Putamen	0.3096	0.2706	0.4111	0.4297
Right Hippocampus	0.5391	0.3222	0.1989	0.3180
RMS Error in Sulci	11.06mm	3.2mm	11.5mm	3.2mm

cortical structures. One of the limitations of this evaluation was that cortical grey matter was not included in the registration since the cortical surfaces were generated by BrainSuite,[31] which selects the inner grey/white boundary as the cortical surface. However, this is a limitation of the preprocessing step rather than the method itself, and the process can be applied to the full cerebral volume provided that a genus-zero brain volume and sulcal labels are supplied. A second limitation is that the cerebellum and brainstem are not included in the analysis since the volume of interest that is mapped is restricted to the cerebrum, bounded by the outer cortical sheet. We can address this issue in practice by modifying the final intensity-based matching step by first adding the brainstem and cerebellum back to the cerebrum. This would also require extrapolation of the deformation field from the harmonic map outwards to these structures as an initialization of the intensity based warp. Alternatively, the cerebellum could also be explicitly modelled using a surface based approach (see, e.g., Hurdal et al.[19]), and its surface and enclosed volume could be treated in a similar fashion to the cerebrum.

7. CONCLUSION

Simultaneous alignment of sulcal features, cortex and subcortical structures is a challenging problem due to variability in the sulcal folding pattern of the cortex. The method presented here based on harmonic maps bridges the gap between surface and volume alignment techniques by extending the surface map to the whole subcortical volume. This allows the large deformation of the sulcal pattern and makes the complex sulcal folds to align accurately, while warping the internal cortical volume bijectively. Through the use of an intermediate spherical map, we are able to constrain the surfaces of the two brain volumes to align while enforcing point matching only at a set of hand labeled sulcal curves. Using harmonic maps we are able to compute large scale deformations between brain volumes allowing cortical surface as well as volumetric intensities to register. This approach combines the strengths of surface registration and volumetric registration methods the ability of surface registration to align surfaces accurately and the ability of volumetric intensity registration to align sub-cortical features.

Acknowledgment

.

REFERENCES

1. G. E. Christensen, S. C. Joshi, and M. I. Miller, "Volumetric transformation of brain anatomy," *IEEE TMI* **16**, December 1997.
2. P. M. Thompson and A. W. Toga, "A surface-based technique for warping 3-dimensional brain," *IEEE Transactions on Medical Imaging* **15**(4), pp. 1–16, 1996.

3. J. Talairach and P. Tournoux, *Co-planar Stereotaxic Atlas of the Human Brain: 3-Dimensional Proportional System - an Approach to Cerebral Imaging*, Thieme Medical Publishers, New York, NY, 1988.

4. J. Ashburner and K. Friston, "Spatial normalization," in *Brain Warping*, A. Toga, ed., pp. 27–44, Academic Press, 1999.

5. R. P. Woods, S. T. Grafton, C. J. Holmes, S. R. Cherry, and J. C. Mazziotta, "Automated image registration: I. General methods and intrasubject, intramodality validation," *Journal of Computer Assisted Tomography* **22**, pp. 139–152, 1998.

6. D. L. G. Hill, P. G. Batchelor, M. Holden, and D. J. Hawkes, "Medical image registration," *Phys. Med. Biol.* **46**, pp. R1–R45, March 2001.

7. G. E. Christensen, R. D. Rabbitt, M. I. Miller, S. C. Joshi, U. Grenander, T. A. Coogan, and D. C. V. Essen, "Topological properties of smooth anatomic maps," in *In 14 Conference on Information Processing in Medical Imaging, France*, pp. 101–112, Kluwer Academic Publishers, 1995.

8. G. E. Christensen, R. D. Rabbit, and M. I. Miller, "Deformable templates using large deformation kinematics," *IEEE Transactions on Image Processing* **5**(10), pp. 1435–1447, 1996.

9. J. Glaunés, M. Vaillant, and M. I. Miller, "Landmark matching via large deformation diffeomorphisms on the sphere," *J. Math. Imaging Vis.* **20**(1-2), pp. 179–200, 2004.

10. B. B. Avants and J. C. Gee, "Shape averaging with diffeomorphic flows for atlas creation," in *ISBI*, 2004.

11. C. A. Pelizzari, G. T. Y. Chen, D. R. Spelbring, R. R. Weichselbaum, and C. T. Chen, "Accurate three-dimensional registration of CT, PET and/or MR images of the brain," *J. Comput. Assist. Tomogr.* **13**(1), pp. 22–26, 1989.

12. N. Krahnstover and C. Lorenz, "Development of point-based shape representation of arbitrary three-dimensional medical objects suitable for statistical shape modeling," in *Proc. SPIE-Medical Imaging 1999:Image Processing*, **3661**, pp. 620–631.

13. J. H. Downs, J. L. Lancaster, and P. T. Fox, "Surface based spatial normalization using convex hulls," in *Brain Warping*, Academic, (San Diego, CA), 1999.

14. T. Hartkens, D. Hill, A. D. Castellano-Smith, D. Hawkes, C. Maurer, A. Martin, W. Hall, and C. T. H. Liu, "Using points and surfaces to improve voxel-based non-rigid registration," in *MICCAI*, pp. 565–572, 2002.

15. C. Davatzikos, J. Prince, and R. Bryan, "Image registration based on boundary mapping," *IEEE Transactions on Medical Imaging* **15**(1), pp. 112–115, 1996.

16. C. Davatzikos and J. Prince, "Brain image registration based on curve mapping," in *IEEE Workshop Biomedical Image Anal.*, pp. 245–254, 1994.

17. S. C. Joshi and M. I. Miller, "Landmark matching via large deformation diffeomorphisms," *IEEE Transactions on Image Processing* **9**, August 2000.

18. G. Gerig, S. Joshi, T. Fletcher, K. Gorczowski, S. Xu, S. M. Pizer, and M. Styner, "Statistics of population of images and its embedded objects: Driving applications in neuroimaging," in *ISBI*, pp. 1120–1123, April 2006.

19. M. K. Hurdal, K. Stephenson, P. L. Bowers, D. W. L. Sumners, and D. A. Rottenberg, "Coordinate system for conformal cerebellar flat maps," *NeuroImage* **11**, p. S467, 2000.

20. M. Bakircioglu, U. Grenander, N. Khaneja, and M. I. Miller, "Curve matching on brain surfaces using frenet distances," *Human Brain Mapping* **6**, pp. 329–333, 1998.

21. P. M. Thompson, M. S. Mega, C. Vidal, J. Rapoport, and A. W. Toga, "Detecting disease-specific patterns of brain structure using cortical pattern matching and a population-based probabilistic brain atlas," in *Proc. 17th IPMI2001, Davis, CA, USA*, pp. 488–501, 2001.

22. A. A. Joshi, D. W. Shattuck, P. M. Thompson, and R. M. Leahy, "A framework for registration, statistical characterization and classification of cortically constrained functional imaging data," in *Lecture Notes in Computer Science*, **3565**, pp. 186–196, July 2005.

23. Y. Wang, M. C. Chiang, and P. M. Thompson, "Automated surface matching using mutual information applied to Riemann surface structures," in *MICCAI 2005, LNCS 3750*, J. Duncan and G. Gerig, eds., pp. 666–674, Springer-Verlag Berlin Heidelberg, 2005.

24. D. Tosun and J. L. Prince, "Cortical surface alignment using geometry driven multispectral optical flow," in *Information Processing in Medical Imaging, LNCS 3565*, pp. 480–492, 2005.

25. D. Tosun, M. E. Rettmann, and J. L. Prince, "Mapping techniques for aligning sulci across multiple brains," *Medical Image Analysis* **8**(3), pp. 295–309, 2005.

26. T. Liu, D. Shen, and C. Davatzikos, "Deformable registration of cortical structures via hybrid volumetric and surface warping," *NeuroImage* **22**(4), pp. 1790–1801, 2004.

27. D. Shen and C. Davatzikos, "Hammer: Hierarchical attribute matching mechanism for elastic registration," *IEEE TRANSACTIONS ON MEDICAL IMAGING* **21**(11), 2002.

28. G. E. Christensen, P. Yin, M. W. Vannier, K. S. C. Chao, J. L. Dempsey, and J. F. Williamson, "Large-deformation image registration using fluid landmarks," in *Image Analysis and Interpretation, 2000. Proceedings. 4th IEEE Southwest Symposium*, pp. 269–273, 2000.

29. H. J. Johnson and G. E. Christensen, "Consistent landmark and intensity-based image registration," *IEEE Transactions on Medical Imaging* **21**(5), pp. 450–461, 2002.

30. R. Hamilton, "Harmonic maps of manifolds with boundary," in *Lecture Notes in Mathematics, 471*, Springer, 1975.

31. D. W. Shattuck and R. M. Leahy, "BrainSuite: An automated cortical surface identification tool.," in *MICCAI*, S. L. Delp, A. M. DiGioia, and B. Jaramaz, eds., *Lecture Notes in Computer Science* **1935**, pp. 50–61, Springer, 2000.

32. F. Mémoli, G. Sapiro, and S. Osher, "Solving variational problems and partial differential equations mapping into general target manifolds," *J. Comput. Phys.* **195**(1), pp. 263–292, 2004.

33. B. Fischl, M. I. Sereno, R. B. H. Tootell, and A. M. Dale, "High-resolution inter-subject averaging and a coordinate system for the cortical surface," *Human Brain Mapping* **8**, pp. 272–284, 1998.

34. P. M. Thompson, M. S. Mega, and A. W. Toga, "Disease-specific probabilistic brain atlases," in *Procedings of IEEE International Conference on Computer Vision and Pattern Recognition*, pp. 227–234, 2000.

35. J. Jost, *Riemannian geometry and geometric analysis*, Springer Verlag, 2002.

36. S. Nishikawa, *Variational Problems in Geometry*, vol. 205 of *Translations of Mathematical Monographs*, AMS, 2001.

37. Y. Xin, *Geometry of harmonic maps*, Birkhäuser, 1996.

38. J. Eells and J. H. Sampson, "Harmonic mappings of Riemannian manifolds," *Am. J. Math.* **86**(1), pp. 109–160, 1964.

39. A. A. Joshi, R. M. Leahy, P. M. Thompson, and D. W. Shattuck, "Cortical surface parameterization by p-harmonic energy minimization.," in *ISBI*, pp. 428–431, 2004.

40. B. Tang, G. Sapiro, and V. Caselles, "Diffusion of general data on non-flat manifolds via harmonic maps theory: The direction diffusion case.," *International Journal of Computer Vision* **36**(2), pp. 149–161, 2000.

41. Y. Wang, X. Gu, and S. T. Yau, "Volumetric harmonic map," *Communications in Information and Systems* **3**(3), pp. 191–202, 2004.

42. P. M. Thompson, K. M. Hayashi, G. de Zubicaray, A. L. Janke, S. E. Rose, J. Semple, D. M. Doddrell, T. D. Cannon, and A. W. Toga, "Detecting dynamic and genetic effects on brain structure using high dimensional cortical pattern matching," in *Proceedings of ISBI*, 2002.

43. R. P. Woods, S. T. Grafton, J. D. G. Watson, N. L. Sicotte, and J. C. Mazziotta, "Automated image registration: II. Intersubject validation of linear and nonlinear models," *Journal of Computer Assisted Tomography* **22**, pp. 153–165, 1998.

44. A. Leow, P. M. Thompson, H. Protas, and S.-C. Huang, "Brain warping with implicit representations.," in *ISBI*, pp. 603–606, IEEE, 2004.

45. F. Mmoli, G. Sapiro, and P. Thompson, "Implicit brain imaging," *NeuroImage* **23**(1), pp. S179–S188, 2004.

46. G. E. Christensen, R. Rabbitt, and M. I. Miller, "3D brain mapping using a deformable neuroanatomy," *Physics in Medicine and Biology* **39**, pp. 609–618, March 1994.

47. V. Camion and L. Younes, "Geodesic interpolating splines," *Lecture Notes in Computer Science* **2134**, pp. 513–527, 2001.

48. Y. Ge, J. M. Fitzpatrick, R. M. Kessler, M. Jeske-Janicka, and R. A. Margolin, "Intersubject brain image registration using both cortical and subcortical landmarks," in *Proc. SPIE Vol. 2434, p. 81-95, Medical Imaging 1995: Image Processing, Murray H. Loew; Ed.*, pp. 81–95, May 1995.

49. P. M. Thompson, C. Vidal, J. N. Giedd, P. Gochman, J. Blumenthal, R. Nicolson, A. W. Toga, and J. L. Rapoport, "Mapping adolescent brain change reveals dynamic wave of accelerated gray matter loss in very early-onset schizophrenia," *PNAS* **98**(20), pp. 11650–11655, 2001.

50. G. E. Christensen, "Consistent linear-elastic transformations for image matching," *Lecture Notes in Computer Science* **1613**, pp. 224–237, 1999.

51. F. L. Bookstein, "Principal warps: Thin-plate splines and the decomposition of deformations," *IEEE Transactions on Pattern Analysis and Machine Intelligence* **11**, pp. 567–585, June 1989.

52. I. Kreyzig, *Differential Geometry*, Dover, 1999.